日本ヒートアイランド学会論文集 Vol.7 (2012)
Journal of Heat Island Institute International Vol.7 (2012)

EVAPORATIVE MIST COOLING OF AN URBAN WASTE-TO-ENERGY PLANT

Craig FARNHAM*[1] Akito TAKAKURA*[2] Masaki NAKAO*[1]
Masatoshi NISHIOKA*[1] Minako NABESHIMA*[1]

*[1] Osaka City University, Dept. of Urban Engineering, Osaka, Japan
*[2] Osaka City Institute of Public Health & Environmental Sciences, Osaka, Japan

Corresponding author: Craig FARNHAM, craig.farnham@gmail.com

ABSTRACT

The City of Osaka has several urban waste-to-energy incineration facilities that both contribute to, and are affected by, the urban heat island. Applying mist evaporative cooling to the forced-draft, air-cooled condensers at these plants can both reduce the exhaust air temperature and increase the amount of electricity produced. The condenser reaches over 70˚C and the exhaust is released at 30m height. Power output drops by over 1%/˚C as air temperatures rise in summer. A misting system was installed over 1/8 of the air intake at a 14.5MW plant. Water droplets with a Sauter mean diameter of 45 microns were sprayed at up to 2.88tons/hr with near-complete mist evaporation. The exhaust air temperature dropped an average of 1.0K. If implemented full-scale, it should yield exhaust temperature reductions of 4-5K. The cooling effect increased the power output by 1.2% for misting periods greater than 45 minutes, but uncertainty is high. Full scale use at all Osaka plants during the summer could increase power generation by 6MW, offsetting 1700 tons of CO_2 per season.

Key Words : Evaporative cooling, Urban heat island, Mist, Power plant, Waste-to-energy

1. INTRODUCTION

The city of Osaka incinerates 97% of its garbage (1) at 9 waste-to-energy plants with a total capacity of 117MW, all located inside the city limits. In summer, the steam cycle forced-draft, air-cooled condenser temperature can reach over 77˚C and the heated air is released at a height of 30m, contributing to the urban heat island. In summer, when electric demand peaks, higher air temperatures cause a reduction in cycle efficiency of the plant, yielding less power output.

Application of mist evaporative cooling at the forced-draft inlet could have two benefits. First, it can reduce the condenser exhaust temperature, countering the contribution to the heat island. Second, the reduction in inlet temperature may reduce the cycle steam condensation temperature and increase power output. The city's water resources can be used to both improve the urban climate and increase energy production.

Spray evaporative cooling has been used as an efficient low-energy cooling technique in dry climates for decades by researchers including Alvarez et al.(2), and Pearlmutter et al. (3) In humid climates such as Japan, evaporative cooling is more problematic. Coarse sprays do not evaporate well, which can result in wetting. Wetting can cause scaling and corrosion. The use of fine mist sprays with average droplet diameters under 50 microns by Yamada et al. (4) and Uchiyama et al. (5) allowed for efficient outdoor cooling without significant wetting. O'Rourke's(6) work provides a thorough explanation of droplet phenomena.

The primary goal of the research is to show that a mist evaporation system can be installed that can generate a spray which will largely evaporate before reaching the power plant's forced-draft condenser and fans. If the spray evaporates, the system can yield significant cooling without need of an extensive refit of the condenser system. Many costs can be avoided; such as increased corrosion reducing equipment lifespan and effectiveness, a need to install mist eliminators, or a need for added drainage or a water recycling system.

The secondary goal was to measure any change in power output of the plant and determine if the potential extra electricity generation can outweigh the price of the system's electricity and water demands.

Takakura et al.(7) made a study of the subject plant power output data for 1 year from Sept. 2007 – Sept. 2008. The data was correlated with weather data from the Osaka city meteorological station[8] located 7km east of the plant. As typical for Rankine cycles, power output drops as the condenser temperature increases [9] as illustrated in Fig. 1. Fig. 2 shows power output expressed in terms of kW per ton of steam through the turbine plotted against air temperature. In this case the best-fit curve shows power drops of more than 1% per degree as air temperatures pass 30˚C. At temperatures around 25˚C, the forced-draft condenser fans start to reach full capacity. There is no ability to improve the cooling of the condenser by increasing fan speed, so power output starts dropping quite sharply.

The normalized root-mean square difference between all data points and the best-fit curve is 2.0% of the power output (0.020*P*). The variation of the data with the best-fit curve is close to that typical for normal distributions, with 73% of the data points within +/-1RMSE, 96% within +/-2RMSE, and 99% within +/-3RMSE. The coefficient of determination (R^2) between the air temperature and power output is 0.63.

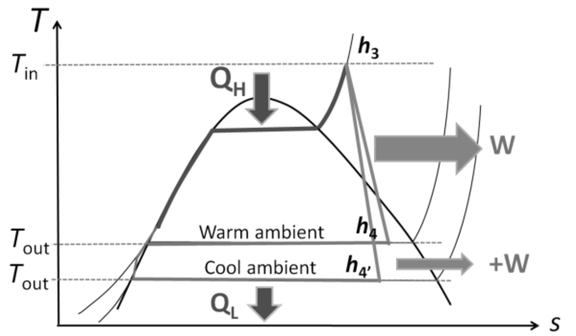

Fig. 1. Rankine cycle with superheat. Increase in turbine output (+W) as temperature of the condenser decreases.

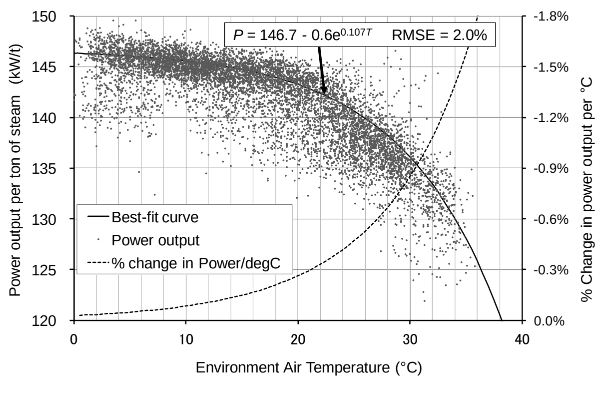

Fig. 2. Power output decreases at higher air temperature.

To show that the power output could quickly change in response to sudden cooling, cases of heavy rainfall were examined in detail. A case of over 30mm/hr of rainfall with air temperature dropping 10K in 1 hour is shown in Fig. 3. From 6:00 to 13:00, the typical summertime power output drop happens as temperatures rise. Then the severe rainstorm occurs. During this time, power output increased by 15%.

Both the 1-year temperature data set and the specific examples of rain lead to an expectation that 1 degree of cooling during hot summer conditions will boost power output by roughly 1%.

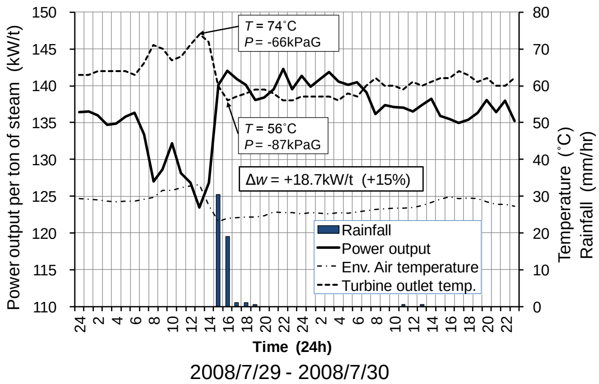

Fig. 3. Change in power output during a period of heavy rain.

1.1 Mist Evaporation

Mist droplets in non-saturated air evaporate, exchanging latent heat with sensible heat from the air, causing the air to cool while becoming more humid. Mist droplet evaporation is typically a quasi-steady state in which the diffusion of vapor away from the droplet is balanced by the flow of heat into the droplet, while the droplet shrinks. Vapor diffusion is expressed in terms of a loss of droplet mass, m_d which is proportional to the difference between the ambient vapor pressure, $\rho_{v,\infty}$ and the vapor pressure at the droplet surface, $\rho_{v,s}$ which is the saturation vapor pressure, as shown in Eq (1).

Flow of heat, q into the droplet is proportional to the difference between the ambient temperature, T_∞ and the droplet surface temperature, T_s as shown in Eq (2). The vapor diffusion and heat transfer are related by the latent heat of evaporation, L in Eq (3).

$$\frac{dm_d}{dt} = 4\pi r D\left(\rho_{v,\infty} - \rho_{v,s}\right) \qquad \text{Eq (1)}$$

$$q = 4\pi r k\left(T_\infty - T_s\right) \qquad \text{Eq (2)}$$

$$q = -L\frac{dm_d}{dt} \qquad \text{Eq (3)}$$

1.2 Significance of the Wet Bulb Depression

Pruppacher and Klett found that the surface temperature of water droplets evaporating in typical atmospheric air conditions is within 0.5K of the wet bulb temperature [10] as in Eq (4). Thus, the temperature difference driving Eq (2) can be estimated as the wet bulb depression, the difference between the ambient dry bulb temperature and the wet bulb temperature, the right-side term in Eq (5). This error is relatively large at low wet bulb depression values (high relative humidity), but the mist evaporation system is not used during periods of high humidity.

$$T_s = T_{WB} \pm 0.5K \quad \text{Eq (4)}$$

$$T_\infty - T_s \approx T_\infty - T_{WB} \quad \text{Eq (5)}$$

By using the ideal gas law and substituting Eqs. (2)~(5) into Eq.(1), an approximation for the evaporation rate of a single droplet, the change in droplet mass d_m over time, can be expressed in terms of the wet bulb depression, here termed ΔT_{WB}.

$$\frac{dm_d}{dt} \approx -\Delta T_{WB} \frac{4\pi rk}{L} \quad \text{Eq (6)}$$

Single droplet evaporation is proportional to ΔT_{WB}. For mist sprays, which are collections of droplets, Farnham et al.[11] found ΔT_{WB} to be a useful single parameter for predicting the mist evaporation rate as a whole, defined as the fraction of mist sprayed that does not collect on a horizontal surface below the misting nozzle. Further, as the coolest temperature that can be produced by evaporative cooling is the wet bulb temperature, ΔT_{WB} is a useful reference as the maximum possible temperature reduction.

When experimenting in various conditions of air temperature and humidity, using ΔT_{WB} as a single parameter allows for easy evaluations of evaporative cooling potential. Higher ΔT_{WB} yields faster and more complete evaporation with greater temperature reductions.

The reduction in air temperature depends on the ratio of the masses of evaporating mist and the air into which it evaporates. In the case of a mist spray of mass flow m_m evaporating, the net heat transfer with the mist, q_m is,

$$q_m = Lm_m Y \quad \text{Eq (7)}$$

where Y is the fraction of the mist spray that has evaporated.

The change in temperature of air, ΔT_a with volume flow V_a and density ρ_a into which the mist evaporates is,

$$\Delta T_a = -\frac{q_m}{V_a \rho_a C_P} = -\frac{Lm_m Y}{V_a \rho_a C_P} \quad \text{Eq (8)}$$

if the mist is uniformly-mixed throughout the affected air. However, mist will likely not be uniformly distributed through the air. Local temperature drops will vary according to the local ratio of mist to air and the evaporation until that point.

1.3 Maximum Evaporable Mist Spray Rate

In saturated air, water mist will not evaporate. If a large enough amount of mist is sprayed into unsaturated air, the air will become saturated as some mist evaporates, then the remaining mist will not evaporate. The absolute humidity of the air would change from the level at the initial state x_0 to the level at the saturated state on a constant-enthalpy line x_{sat} as it is a constant-enthalpy process. This change in absolute humidity can be expressed as,

$$\Delta x = x_{sat} - x_0 \quad \text{Eq (9)}$$

The moisture for this change in humidity comes from the evaporated mist. Thus, the maximum amount of mist that can evaporate into the air is equal to this Δx. Adapting this to a forced draft of air with volume flow V_a and dry air density ρ_{da}, the maximum evaporable mist spray rate m_{max} is,

$$m_{max} = V_a \rho_{da} \Delta x \quad \text{Eq (10)}$$

Both the change in air temperature ΔT_a and the change in absolute humidity Δx due to evaporation are directly proportional to the amount of mist evaporated, as shown in Eq (8) and Eq (10), respectively. Therefore in the case of complete evaporation, the ratio of the change in air temperature to the maximum possible temperature change (ΔT_{WB}) is proportional to the ratio of the mist sprayed to the maximum evaporable mist spray rate.

$$\frac{\Delta T_a}{\Delta T_{WB}} = \frac{m_m}{m_{max}} \quad \text{Eq (11)}$$

Applying Eq (11) to an example, if the forced-draft inlet air conditions are such that ΔT_{WB} is 10K, and 10% of the maximum evaporable spray rate as determined by Eq (10) is sprayed into the air in an otherwise adiabatic process, the average temperature drop in the area where the mist has completely evaporated should be 1K.

1.4 Single Droplet Evaporation Time

Using the single droplet evaporation rate as given in Eq (6), the time needed for the droplet to completely evaporate can be calculated. Assuming the mass of a single droplet moving through air is too small to change the condition of the surrounding environment, the wet bulb depression is a constant.

Droplets falling in air with diameters under 280μm can be assumed as spheres.[12] With all mist droplets as spheres with the density of water, the evaporation equation can be put in terms of a change in droplet radius.

$$\frac{dm_d}{dt} = \frac{dm_d}{dr}\left(\frac{dr}{dt}\right) \quad \text{Eq (12)}$$

$$4\pi r^2 \rho_w \frac{dr}{dt} \approx -\Delta T_{WB} \frac{4\pi rk}{L} \quad \text{Eq (13)}$$

$$r\frac{dr}{dt} \approx -\frac{\Delta T_{WB} k}{L\rho_w} \quad \text{Eq (14)}$$

The radius and time variables can be separated and the resulting equation integrated to yield the equation for droplet radius as a function of time, r_t.

$$\int_{r_t}^{r_0} r\,dr \approx -\int_t^0 \frac{\Delta T_{WB} k}{L\rho}\,dt \quad \text{Eq (15)}$$

$$r_0^2 - r_t^2 \approx \frac{2\Delta T_{WB} k}{L\rho} t \quad \text{Eq (16)}$$

This is sometimes known as the D^2 *law* (diameter square law) of droplet evaporation. [13] Complete evaporation occurs when the radius reaches zero. Substituting zero for r_t yields the equation for time to complete evaporation, t_{ev}.

$$t_{ev} \approx \frac{L\rho r_0^2}{2\Delta T_{WB} k} \qquad \text{Eq (17)}$$

Plotting this for several values of wet bulb depression yields a quick reference chart, Fig. 4. This shows what should be the best-case (fastest) droplet evaporation time. As mist evaporates, the wet bulb depression will decrease as the air becomes cooler and more humid, increasing evaporation times.

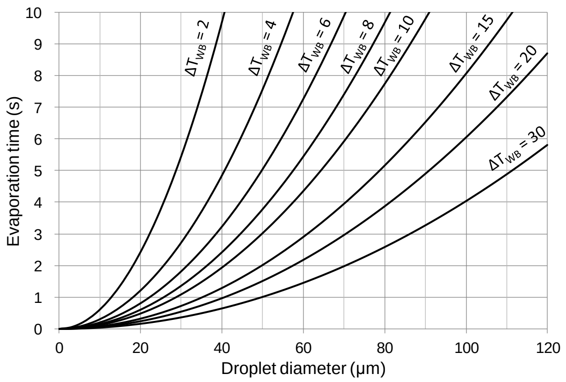

Fig. 4. Time to complete evaporation for single droplets of water in unchanging air conditions.

2. METHODS AND EQUIPMENT

2.1 Power Plant, Misting Equipment and Method

The Nishiyodogawa waste incineration plant can generate 14.5MW of electricity. The plant condensers handle an average of 70 tons/hr of steam from the turbine. The turbine inlet conditions are held at 271˚C +/-2˚C and 2100kPag +/-10kPag, with the steam mass flow varying from 33 to 90ton/h, with an average at about 70ton/h. In summer, the turbine exit conditions typically vary over a temperature range from 43˚C to 77˚C and pressures from -95kPag to -64kPag.

The forced-draft for the plant's two main condenser units is generated by 16 fans of 6m diameter with a capacity of 8770m^3/min each. The air intake is a walled-off section on the north side with an open roof cross-sectional area of 400m^2 as shown in Fig. 5. The cross-sectional area of the outlet above the condensers is 700m^2. Air velocity at the fans running at capacity was measured with a hot-wire anemometer at about 3m/s with high spatial variability due the many obstructions (support columns, beams, catwalks, etc,). In summer temperatures over 25˚C, the fans always run at full speed, which should yield an average upward air velocity of 3.3m/s across the outlet plane.

The condensers are large banks of aluminum fin tubes. The fins are 5cm in diameter. The tubes are about 10m long, oriented diagonally, with steam entering from a header at the apex of the 2 fin tube banks splitting to both sides, and condensate flowing out the bottoms and routed to a condensate tank. The fin tubes are adjoining and stacked 4 layers thick.

The misting system consists of 156 hydraulic nozzles that spray droplets at 5MPa with a SMD (Sauter mean diameter) of 45μm. The droplet diameter distribution (in 2μm bins) and CVF (Cumulative Volume Fraction) as measured by a PDPA (Phased Doppler Particle Analyzer) at a point 50cm from a nozzle at the centerline are shown in Fig. 6. The CVF expresses the portion of the total volume of the entire spray accounted for by droplets of the indicated size or lower. Here, the CVF is 0.9 at 95μm, thus 10% of the spray volume is relatively large droplets over 95μm. In preliminary experiments, these nozzles showed mist evaporation rates of 85-100% (complete evaporation) for freefall heights of 15m-25m, depending on air conditions.

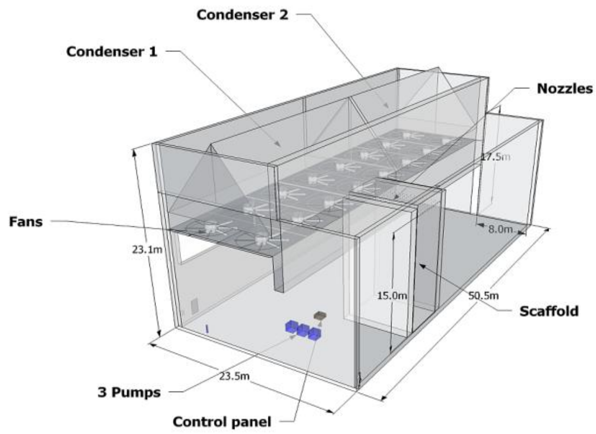

Fig. 5. Layout of the condensers, air inlet section, and installed misting system.

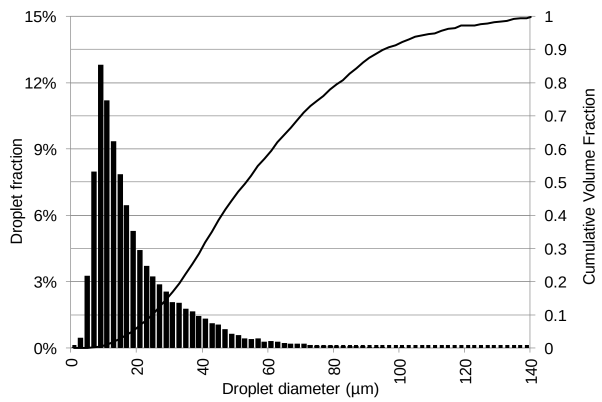

Fig. 6. Nozzle droplet diameter distribution (in 2 μm bins) and cumulative volume fraction.

Three high-pressure water pumps drawing 4kWe each supplied a total 2.88 tons/hr of mist spray. This is about 14-23% of the maximum evaporable mist spray rate as determined by Eq (10) for the range of inlet air conditions. The pumps can be turned on and off individually, to allow spraying of about 1/3 or 2/3 of the maximum with some variability. The total flow rate of water was measured for each pump on/off combination at the water main with a mechanical flow meter.

Experiment trials were done by spraying at a constant flow rate for periods of 30, 45, 60 or 120 minutes. All 3 pumps were started simultaneously and stopped simultaneously at the end of the period. It took about 15 seconds from activation until the spray became steady. In 1 case (noted in Results) the total amount sprayed was lower than desired, due to trouble with the water supply.

The mist nozzles were mounted in a 50cm grid covering a 6m x 8m section of the air intake at a height of 15m. Nozzles were oriented straight down. The installation was temporary, with scaffolding left in place to allow access to the nozzles. This is shown in Photo 1.

Photo 1. Nozzle array during spraying. Photo taken from below. Note scaffolds at left and right, and structural beams in center which capture some of the mist

The flow of mist is directed by the flow of air through the condenser area as shown in Fig. 7. Inlet air (straight blue arrow) from above passes the nozzles and is drawn (curved blue arrow) through the open space (9m height) into the fans. Warmed outlet air (red arrows) is blown upward, with some short circuiting (curved red arrow). The amount of short circuiting, likely influenced by changes in the ambient wind speed and direction, may account for the high variability in air inlet and outlet temperatures, and even the power output.

The mist array directly covers about 1/4 of the inlet area for 1 condenser unit, but spreads to enter 6 of the 8 fans, shown in Fig. 8 as “Mist area”. If all the mist evaporates it should yield 1960kW of cooling as per Eq (3). The air flow through each fan requires 177kW of cooling to reduce the temperature 1K. Thus, if the mist spreads evenly to all 8 fans with complete evaporation at maximum spray, the average cooling should be 1.4K as per Eq (8). If the mist spread evenly to only 6 fans as shown in Fig. 8, there should be a 1.8K temperature drop. According to the power output and weather correlations as shown in Fig. 2 and Fig. 3, this is expected to yield roughly a 1% increase in power output.

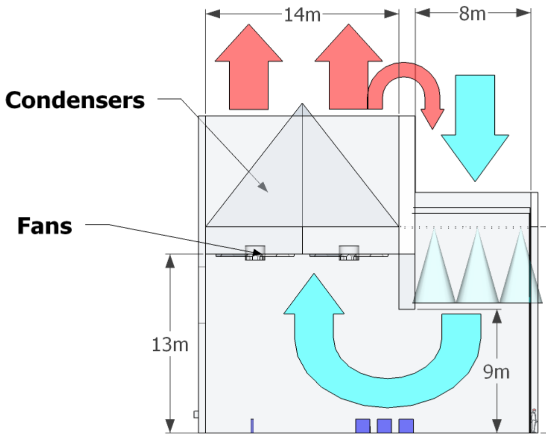

Fig. 7. Cross-section of plant condenser area and nozzle position. Arrows indicate flow of air and mist.

2.2 Sensors

The effect of the mist on the air was measured with both T-type thermocouples and platinum-resistance temperature / capacitive-chip humidity sensors. Sensors were placed 3m above the misting nozzles, 1m above and below the condenser unit in the path of the mist, and at the condenser region farthest from the mist. Thermocouples placed above the condenser were rigged as 4 in parallel and the average reading taken to counter any spatial variation in temperature between the individual fin tubes. Sensor locations are shown in Fig. 8 and Fig. 9 with an explanation of the chart abbreviations and locations in Table 1. An example of sensor mounting onto the condenser is shown in Photo 2.

2.3 Mist Evaporation Rate

Observations of misting test runs showed that the sprayed water would be in one of the following states after the end of spraying.

- Collected at ground level, some draining away and some evaporating away.
- Adhering to an obstruction (scaffold, beams, screens, fans) with some portion dripping to the ground and the rest eventually evaporating.
- Completely evaporated without adhering to any object.

Observation of the space between the fans and the condenser fin tubes including the underside (windward side) of the fin tubes while in operation was not permitted for safety reasons. No mist was visible passing through the condenser on the outlet side. No wetting was seen on the outer, visible side of the fin tubes nor on the sensors placed there.

It is possible that there were some drops passing through the condenser, but their number too small to be noticed visually. If droplets survived to pass the fin tubes, they would evaporate quickly in the 60˚C-70˚C air. For example, according to droplet evaporation times in Fig. 4 for the typical observed outlet air conditions with a ΔT_{WB} of about 30K, even a 100μm droplet would likely evaporate in 4 seconds. As the average wind speed through the condenser is 3m/s, this would mean evaporation about 12m above the condenser.

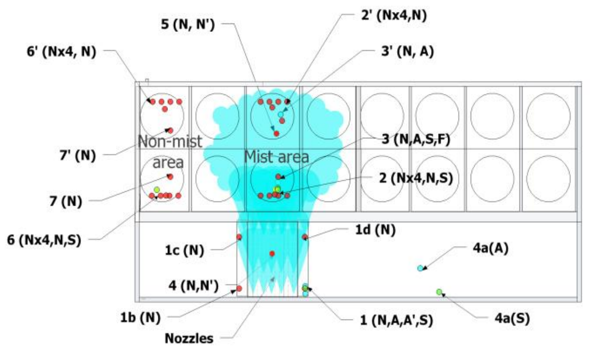

Fig. 8. Layout of the sensors (Top view, locations not to scale)

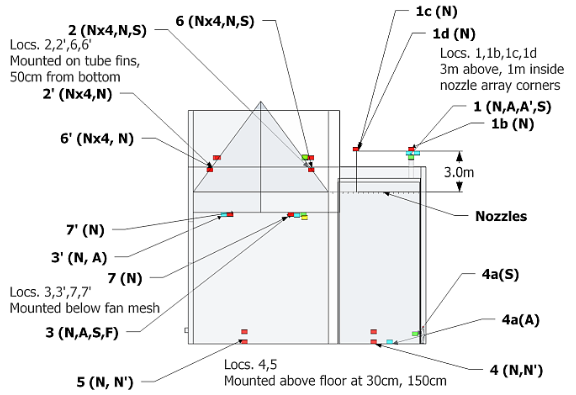

Fig. 9. Layout of the sensors (Side view, locations not to scale)

The effect of evaporation depends on where and when it occurs. Evaporation before or in contact with the condenser can contribute to reducing the condenser temperature and possibly increasing power output.

Evaporation after passing through the condenser would still have value in reducing the sensible heat load from the condenser as a heat island countermeasure. Further, it may still have some effect on power output, as there is some short-circuiting of the outlet air back into the inlet.

During misting and after misting is stopped, evaporation from wetted surfaces will provide a delayed cooling effect.

Thus, it can be thought that the only "waste" is when mist water collects in large enough amounts to make its way to floor drains and exit the experiment area before evaporating.

Table 1. Sensor layout: Types and measurements.

Loc.	Sensor code (Qty)	Measurement target
1	S,A,N(4)	Environment above nozzles, Possible short circuit air flow effect
2	S,N,N x 4	Condenser outlet in misting zone, Side near mist
2'	N,N x 4	Condenser outlet in misting zone, Side far from mist
3	S,A,F,N	Condenser inlet below fans in misting zone, Near mist
3'	A,N	Condenser inlet below fans in misting zone, Far from mist
4	N(2)	Floor level below nozzles
4a	S,A	Environment conditions 20m away from experiment area
5	N(2)	Floor level below fans, 30cm and 150cm height
6	S,N,N x 4	Condenser outlet in no-mist zone, Side near mist
6'	N,N x 4	Condenser outlet in no-mist zone, Side far from mist
7	N	Condenser inlet below fans in no-mist zone, near mist
7'	N	Condenser inlet below fans in no-mist zone, far from mist

Sensor Code	Description
A	Rain/wetness sensor
F	Anemometer (ultrasound, 3D)
N	T-type thermocouple
Nx4	4 T-type thermocouples in parallel
S	Temperature/humidity sensor in non-ventilated shelter (wind speed at measurement locations is about 3m/s)

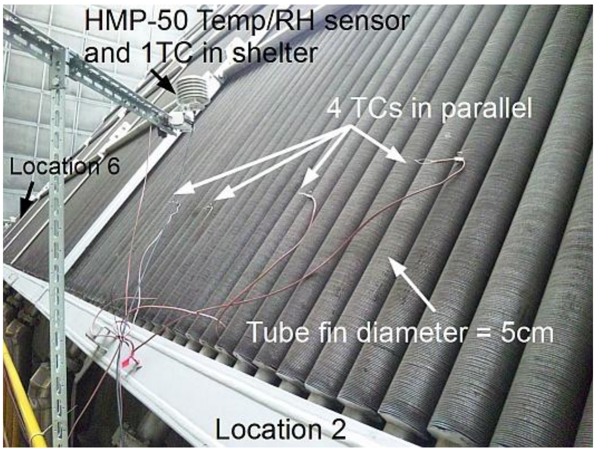

Photo 2. Sensors at Location 2. Thermocouples (TCs) in parallel to average out local differences among fin tube temperatures. Location 6 visible in background at left.

Here, the "mist evaporation rate" is meant to measure the amount of water that would not collect in significant amounts at ground level to drain way as "wasted" mist. It was measured by collecting the unevaporated spray which fell to ground level, either directly from the nozzles or after dripping from obstructions. Twenty 0.4m^2 plastic trays were regularly spaced across the spray area to collect the fallen spray for a set period.

The trays were covered within 1 minute of the end of the misting period to reduce evaporation of the collected water. This is a trade off, as it prevents capturing of delayed dripping from obstructions. However, the amount of this dripping after misting stopped was not large enough to be significant except under the rig scaffolding (including safety nets) which tended to capture the mist and become soaking wet. Thus, the captured mist data is divided into two types (in Table 2 in the Results section) to account for this difference.

The unevaporated water per unit area was interpolated over the visible spray area and compared to the amount of water sprayed. Evaporation rate measurements were labor-intensive and could not be performed for all misting cases.

2.4 Power output data

Power output data was provided in the form of separate coarse, color graphic printouts with 1 pixel representing 0.06MW of electric generation and 0.3 ton/hr of cycle steam. The printouts were scanned and converted into numerical data using the software *WinDIG* created by Lovy[14]. Assuming the software yields accuracy to within 1 pixel of the coarse printout, the resulting error in power output per ton of steam is 1.4kW/ton, which is about 1% of the total. This poses a problem, as the expected power increase per ton of steam is about 1%. Evaluating power output by comparing several periods with misting and several periods without misting from data scanned and converted in the same way should reduce the influence of any bias due to data scanning.

Further, plant staff neglected to print out the power output logs after some experiments and the data was lost. This meant that some evaporation rate measurements could not be correlated with power output data.

3. RESULTS

3.1 Mist Evaporation Rate

The fraction of the mist that evaporated before reaching the fans, or the area between the fans and condenser was unknown. Due to evaporation form surfaces and dripping, and the fact that the wind was blowing upward, there was no way to reliably measure the amount of mist reaching the fan area. Plant operations (including fan speed) could not be adjusted or stopped for the purpose of the experiments, neither for initial installation of equipment nor during the trials.

During trials, the fan unit motor (motors are below the fans, thus upwind and exposed to the mist) and much of the access catwalk for the 1 fan closest to the mist nozzles became noticeably wet with some dripping water in most experiments, except when ΔT_{WB} was 10K or above.

It was possible to capture and measure the amount of mist that reached the floor or dripped to the floor from obstructions. This mist "wasted" to the floor could drain away and its evaporative cooling effect lost. The inner area immediately beneath the misting nozzle headers tended to become quite wet as mist hit the temporary scaffold and nozzle piping and dripped below. If the system were permanently installed, there would be no scaffold. In the outer area beyond the scaffold, under the condensers, less mist collected. In this case, much of the collected water was drops falling from obstructions in the path of air flow. These results are separated in Table 2. "Mist waste to floor - In" is the water captured under the scaffold. "Mist waste to floor - Out" is the water captured outside the scaffold area, under the condenser fans. Both are included in calculations of the net evaporative cooling.

This data shows that on average about 94% of the mist did not collect on the floor as wasted mist, and implies that if there were no scaffold, the rate would be over 98%.

At first glance, the mist waste amounts seem to have no clear correlation to experiment parameters. This could be explained by two competing influences.

Table 2. Unevaporated mist collection rate and expected evaporative cooling.

Date Time	Mist time	ΔT_{WB}	Mist	Mist "waste" to floor (%)		Evap. Cooling
	Min	K	t/hr	In	Out	kW
8/24 13:33	120	8.5	2.89	10.4	2.1	1720
8/23 13:43	60	6.3	2.89	9.2	1.4	1760
8/24 10:58	60	6.5	2.89	4.3	0.6	1870
8/18 13:41	60	10.2	2.30	0.2	2.2	1530
7/27 11:42	60	9.7	2.89	4.5	1.4	1850
7/27 16:10	60	9.4	1.84	1.6	1.0	1220
7/28 10:03	60	5.7	1.84	3.5	1.4	1190
8/13 11:12	60	6.2	1.83	0.9	0.9	1220
8/25 13:59	30	7.4	2.89	1.0	0.2	1940
8/25 15:10	30	10.0	2.89	0.4	0.1	1960
8/13 13:35	30	6.8	1.81	1.5	2.9	1180
Time-weighted avg.				4.4	1.2	1620

The percentage of mist collected should tend to increase as misting time increases. More spray will yield more wetting of surfaces, and more dripping into the collection trays. Water pooling in the trays or on the floor will evaporate much more slowly than mist in droplet form, due to the much lower ratio of surface area to mass. Conversely, a very short spray period could yield almost no surface wetting, or wetting with quick evaporation, and no water collected in the trays.

The percentage of mist collected should also tend to increase with a higher evaporable mist ratio m_m/m_{max} due to increasing saturation of the air. More droplets will survive to adhere to the floor and other surfaces. Water on wetted surfaces will evaporate more slowly, with greater tendency to collect and drip to the floor.

Collected mist rates should be proportional to the ratio

m_m/m_{max} and to total spray time t_{spray}. We can combine these two into a single parameter, which we term B, with units of time (see Table 3). This would be the amount of time it would take to spray the same amount of mist if the mist flow rate were increased to the maximum evaporable mist spray rate m_{max}.

$$B \equiv \frac{m_m}{m_{max}} t_{spray} \qquad \text{Eq (18)}$$

Plotting B against the values of collected mist fraction, a good correlation, with a coefficient of determination of 0.75, is apparent (see Fig. 10). The best-fit line has a y-intercept at about 4 minutes. This matches the expectation that short bursts of spray could yield no collected mist. This suggests that if total mist flow and spray time is limited to keep parameter B under 4 (for example, spraying for 20 minutes at m_m/m_{max} = 1/5) in a single spraying period, mist might not collect on the floor. It is possible no water would be lost down the drain.

Table 3. Correlation of total wasted mist with parameter B

Date Time	Mist time	ΔT_{WB}	Mist	Total mist "waste", F	B
	Min	K	t/hr	%	min
8/24 13:33	120	8.5	2.89	12.5	13.8
8/23 13:43	60	6.3	2.89	10.6	20.9
8/24 10:58	60	6.5	2.89	4.9	13.1
8/18 13:41	60	10.2	2.30	2.4	5.9
7/27 11:42	60	9.7	2.89	5.9	4.3
7/27 16:10	60	9.4	1.84	2.6	6.7
7/28 10:03	60	5.7	1.84	4.9	9.0
8/13 11:12	60	6.2	1.83	1.8	5.9
8/25 13:59	30	7.4	2.89	1.2	9.6
8/25 15:10	30	10.0	2.89	0.5	8.9
8/13 13:35	30	6.8	1.81	4.4	4.0

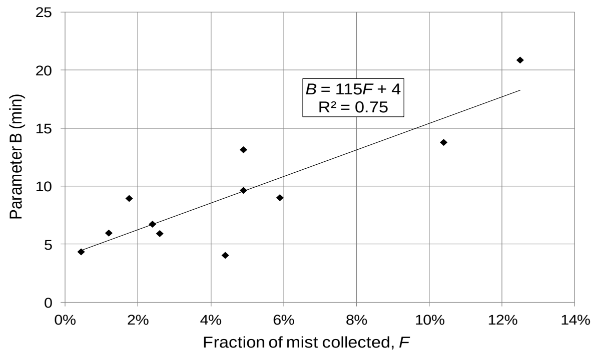

Fig. 10. Trend of amount of mist collected in proportion to parameter "B"

With further investigation into drying times, and the influence of the thermal mass of the obstructions and floor on flash evaporation of the initial portion of droplets contacting them, this type of parameter could have value in determining limits on misting time and spray amounts based on the air conditions to reduce wetting of surfaces and wasting mist spray to drainage by using intermittent spraying.

The latent heat of the evaporated mist yielded an average of 1620kW of cooling, nearing a maximum of 2MW. If scaled up this could yield 16MW of cooling, a significant fraction of the heat of condensation for the typical 70tons/hr of steam in the cycle, which is about 45MW. The 1620kW of cooling should yield an average temperature drop at the outlet of 1.5K if spread across 6 fans.

3.2 Mist Cooling Temperature Drops

During misting, the sensors below the condenser at the forced-draft fan intake on the side closest to the mist (Location 3) tended to become wet. An example case of the temperature and relative humidity data from the sheltered temperature /humidity sensors for Location 3 and for the outlet area above the condenser (Location 2) are shown in Fig. 11. The wet bulb temperature calculated at the inlet (Location 1) sensor data is included. The Loc. 3 sensor temperature dropped to around the wet bulb temperature for most of the 60 minute misting trial. The relative humidity reading neared 90%. During this trial and after, the sensor shelter was visually confirmed as wet. Using this sensor data as representative of the entire misted area would yield temperature drops much larger than the expected 1.0K – 1.8K drop, thus they are not used to evaluate the temperature drops here.

On the other hand, the sensors at Location 2 did not visually appear wet, and the sensor data seems to indicate they did not become wet. Relative humidity only slightly exceeded 15% during the misting period. Further, the wet bulb temperature of the outlet air as measured before the misting period is typically about 35˚C, whereas the measured outlet temperature never dropped below 50˚C in any of the measured cases. However, it is possible that the sensors were being slightly wetted by droplets which evaporated too quickly to accumulate to a level that would be visible, nor to yield a wet bulb type effect. The temperature readings above the condenser are used to evaluate the cooling effect here.

During misting, readings of the sheltered temperature/ humidity sensor above the condensers showed a difference arises between temperatures of the misted area (Location 2) and the no mist area (Location 6), such as in the example case shown in Fig. 12. The average temperature differences for all trials are given in Table 3, with all cases showing some temperature reduction. The average of all cases is 1.0K, but is based on the assumption that the mist cooling did not affect the sensors farthest from the mist. If the cooling effect spread to those sensors as well, the actual temperature drop should be even larger.

Fig. 13 shows the trend of this temperature difference over time for the 30 minute misting trials (longer trials show the same trend). The cooling effect reaches a maximum about 10 minutes after spraying begins, and returns to zero about 10-15 minutes after it stops. This delay may be due to the large mass of the condenser unit, estimated at 90 tons. As the cooling effect of the mist ends about 10-15 minutes after misting is stopped, in calculations of relative power output change (Section 3.3), it is assumed that the power output at 15 minutes after misting stops represents what the power output would be if there had been no misting.

The measured temperature drop is lower than the expected value as determined by the evaporation rate. This may be due to the sensor location. Sensors were not installed at multiple locations across the condenser to get a complete spatial distribution of temperature.

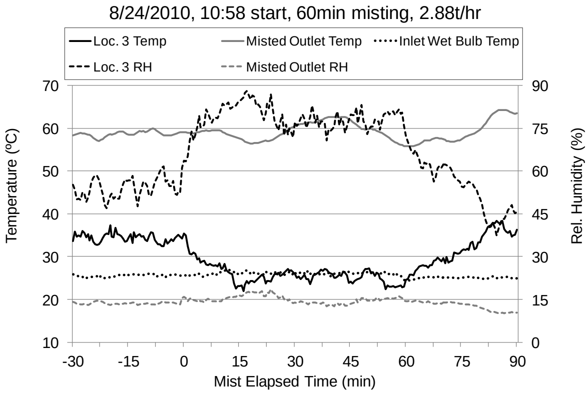

Fig. 11. Temperature and Rel. Humidity in the misted area at the outlet (Loc. 7) and below the condenser fans (Loc. 3) where sensor wetting clearly occurred.

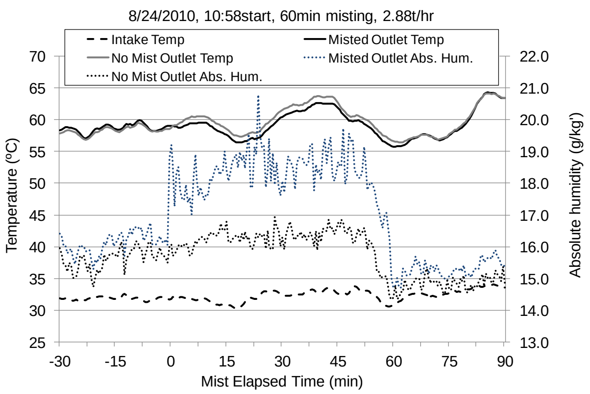

Fig. 12. Example case of temperature and abs. humidity above condenser in the misted area and no-mist area during a 60-minute trial.

3.3 Change in Power Output

Evaluating power output changes was problematic, as plant operating conditions could not be held constant for the purpose of the experiment. Steam conditions depended on the amount of garbage being burned and many other operational factors. During some misting trials, cycle steam was vented directly below the condensers. Further, weather conditions (temperature, relative humidity, wind direction, wind speed, sunlight, clouds, etc.) change during the misting period.

In the previous study, there was no clear correlation of these factors with power output beyond the general temperature trend in Fig. 2. It is assumed the RMSE of 2.0% with the best-fit curve is due to all the other factors, and a similar variability was expected in results for power output changes due to mist cooling.

Table 4. Difference in temperature of misted and non-misted areas above the condenser.

Date & Time (2010)	ΔT_{WB}	Misting	Meas. ΔT	Expected ΔT, 6 fan spread
	K	min	K	K
8/24 13:33	9.1	120	-1.4	-1.6
8/24 10:58	6.2	60	-1.2	-1.8
8/23 13:43	6.7	60	-1.5	-1.7
8/18 13:41	10.5	60	-0.3	-1.1
8/25 15:10	6.7	30	-1.1	-1.5
8/25 13:59	6.4	30	-1.3	-1.8
7/28 14:08	11.1	60	-0.9	No evap. rate data
8/18 15:01	11.5	45	-0.4	
8/18 16:06	12.0	30	-0.4	
8/23 15:24	7.0	30	-0.9	
8/4 13:29	9.4	30	-1.0	
7/28 16:05	6.7	30	-1.0	
8/4 14:25	8.8	30	-1.2	
8/4 10:50	9.9	30	-0.5	
Average of cases			-0.9	-1.6
Time-weighted average			-1.0	-1.6

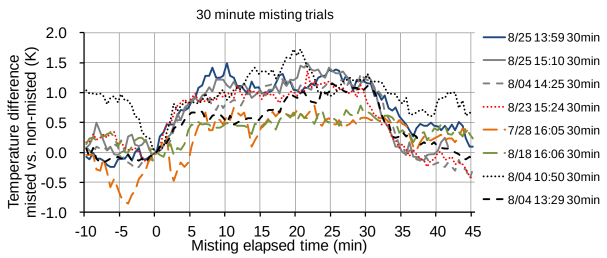

Fig. 13. Temperature differences arising between misted and non-misted areas at outlet during misting.

A plot of power output (see Fig. 14) smoothed by a 6-minute time averaging (which smoothes the periodic variation due to the garbage stoking frequency) still shows the output varies by about 3% during a 60 –minute misting trial.

A method was developed to evaluate the change in power output by creating a hypothetical non-misting power output line. The average power output at the start of misting cannot have been affected by mist. Further, temperature and humidity data typically returned to initial values about 10-15 minutes after misting was stopped. Therefore, it is assumed that the power output data 15 minutes after misting is also not affected by mist. Connecting these points yields a hypothetical non-misting line. Power output is expected to vary above and below this line in the typical manner if there had been no misting. The difference between the recorded power output and this hypothetical line is taken as the effect of the misting on power output. Integrating the difference yields the total power output change. Integration was only done over the misting period.

A single trial showing a net power increase could be just random chance, but a trend to positive results over many trials could indicate that misting was effective. If there is no effect from the mist, the average of all trials should be near zero.

The method was also applied to random selections of data from non-misting periods to test for bias, with an example of the curve integration yielding almost no net change given in Fig. 15. The average of the non-misting cases was a 0.09% increase, with a standard deviation (SD) of 1.0%. These bias check results are in Table 5.

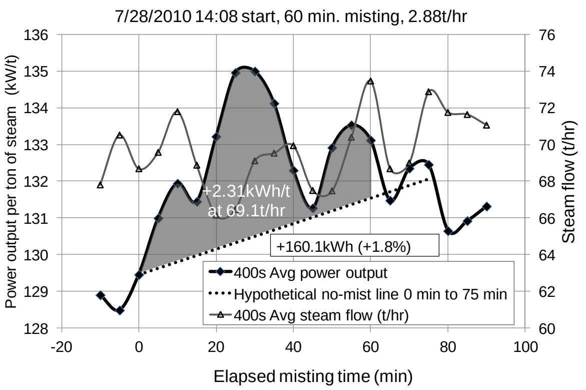

Fig. 14. Example of difference between time-averaged actual power output (solid line) and hypothetical non-misting (dotted line). Area under the curve represents the total power increase.

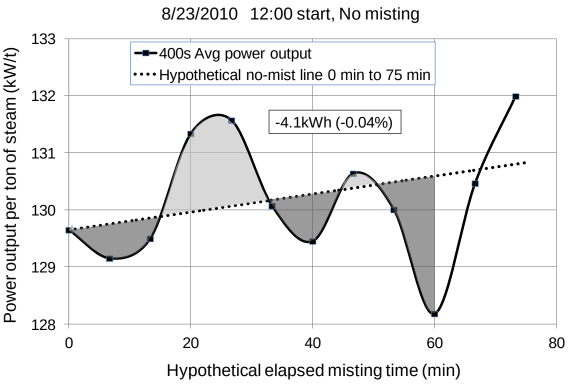

Fig. 15. Example of check for bias using the integration method for a period without misting.

Table 6 shows the results for all trials. 11 cases show some increase in power, and 3 cases show a decrease. All cases of longer spray periods (45 minutes or more) show power increases, with the longest spray period (120 min) being the second best. The SD of percent power increase is larger than the average increase, giving low confidence in the result. However, for cases of longer-period misting, the average (+1.2%) is nearly 2 SD (0.65%) above the non-misting average (+0.09%).

Setting the endpoints of the hypothetical non-mist line to the mist start time and the mist end time, rather than 15 minutes later, yielded the same trend of increased power output, with the same 3 cases of decreased output, shown in Table 7. The time-weighted average increase became +0.7% for the longer-period misting. A lower increase is expected, as delayed cooling effects remaining after misting was stopped are not compensated for.

Table 5. Test for bias in integration method by applying to non-misting periods

Date & Time	Period	Change in output	
	min	kWh	%
8/4 15:30	30	+15	+0.3%
8/4 12:10	30	-26	-0.6%
8/23 12:00	30	+5	+0.1%
8/23 12:10	30	+105	+2.2%
8/23 12:20	30	-27	-0.6%
8/18 12:05	30	-28	-0.5%
8/4 15:30	60	+109	+1.2%
8/4 12:10	60	+141	+1.6%
8/23 12:00	60	-44	-0.04%
8/23 12:10	60	+18	+0.2%
8/23 12:20	60	-125	-1.3%
8/18 12:05	60	-61	-1.2%
	Average	+13.4	+0.11%
	Time-weighted average	+11.0	+0.09%

Table 6. Inlet air conditions and changes in power output calculated by the integration method (from time zero to 15 minutes after misting).

Date & Time (2010)	Inlet		Mist	Change in output	
	Temp	RH			
	˚C	%	min	kWh	%
8/24 13:33	34.1	48	120	+337	+1.7
7/28 14:08	36.5	41	60	+160	+1.8
8/24 10:58	31.8	61	60	+123	+1.3
8/23 13:43	32.8	59	60	+107	+1.2
8/18 13:41	35.5	43	60	+4	+0.1
8/18 15:01	36.2	39	45	+12	+0.2
7/28 16:05	32.4	59	30	+57	+1.2
8/4 14:25	35.0	50	30	+42	+1.0
8/4 10:50	34.9	45	30	+38	+0.8
8/25 15:10	32.6	59	30	+28	+0.6
8/18 16:06	37.0	38	30	+17	+0.4
8/23 15:24	33.2	58	30	-12	-0.3
8/4 13:29	34.6	47	30	-29	-0.7
8/25 13:59	32.1	60	30	-103	-2.0
Time-weighted avg				+102.0	+0.8
Misting >= 45 min Time-wtd. avg				+159.6	+1.2
Standard Dev. mist					0.94
Standard Dev. Mist>= 45 min					0.65
Avg. No-mist bias check					+0.09
Standard Dev. No-mist bias check					1.04

Though the result agrees with the expectations that there would be about a 1% increase in power output, the uncertainties are too large. The integral method result's SD is also about 1% of power output, while the variance in the relationship between power output and air temperature itself has a RMSE of about 2% (see Fig. 2). This experiment is not definitive proof that misting increased power output in these cases. But the average of all cases indicates a positive trend, in agreement with theory.

If the trend is true, the average power increase of 102kW is over 8 times the power demand of the water pumps. If sold at 10 yen/kWh, with the cost of water at 100 yen/m^3, the net gain is 600 yen per hour of operation, or 540,000 yen/season if operated 10 hours/day for 3 months at the 1/8 size trial scale.

Table 7. Inlet air conditions and changes in power output calculated by the integration method (from time zero to mist stop)

Date & Time (2010)	Inlet Temp ˚C	Inlet RH %	Mist min	Change in output kWh	Change in output %
8/24 13:33	34.1	48	120	+198	+1.0
7/28 14:08	36.5	41	60	+107	+1.2
8/24 10:58	31.8	61	60	+12	+0.1
8/23 13:43	32.8	59	60	+1	+0.0
8/18 13:41	35.5	43	60	+52	+0.1
8/18 15:01	36.2	39	45	+12	+1.0
7/28 16:05	32.4	59	30	+37	+0.8
8/4 14:25	35.0	50	30	+38	+0.9
8/4 10:50	34.9	45	30	+44	+1.0
8/25 15:10	32.6	59	30	+59	+1.4
8/18 16:06	37.0	38	30	+2	+0.1
8/23 15:24	33.2	58	30	-84	-1.8
8/4 13:29	34.6	47	30	-20	-0.5
8/25 13:59	32.1	60	30	-145	-3.2
Time-weighted avg				+50.4	+0.4
Misting >= 45 min Time-wtd. avg				+85.5	+0.7
Standard Dev. mist					1.22
Standard Dev. Mist>= 45 min					0.46
Avg. No-mist bias check					+0.09
Standard Dev. No-mist bias check					1.04

4. DISCUSSION AND CONCLUSIONS

An evaporative mist cooling system spraying up to 2.88 tons/h of droplets with a SMD of 45μm was installed at the inlet of an air-cooled condenser of a steam turbine power plant to evaluate the effects. The mist spray flow was about 14-23% of the maximum possible spray flow that could evaporate in the range of air conditions. The system covered 1/4 of the inlet area of 1 of the 2 plant condensers, but the mist diffused to cover about 3/4 of the inlet area at the intake fans. Spray periods ranged from 30 – 120 minutes.

Although the mist appeared to have completely evaporated at the condenser outlet with no signs of wetting nor visible droplets, there was some wetting of the fans, floor, and surfaces below the condenser. Wetting of the floor averaged about 6% of the sprayed mass. If the nozzles were placed at a greater height, and temporary scaffolds removed, better evaporation should result. Correlation of wetting with duration and amount of mist sprayed indicates that intermittent spraying could also reduce or eliminate water "wasted" to the floor and drains. The evaporative cooling at 1/8 scale can yield up to about 2MW of cooling and an average temperature drop of 1.0K over 1 condenser unit. If scaled up, this could yield 16MW of cooling and a drop of 4-5K. This would counter about 30% of the exhaust heat from cycle steam condensation at this plant.

In these trials, power output was increased by the expected 1%, though uncertainties in the data are large. The average power increase from longer-term misting over 45 minutes is nearly 2 standard deviations above the null case. If scaled up, the power increases could exceed 5%. If so, full-scale use at all such plants in Osaka could yield 6MW of additional power, and offset 1700tons of CO_2 from other plants per season. Further trials would be better served by more modern plant monitoring and logging equipment, and the ability to control plant operations for the purposes of the experiment.

5. NOMENCLATURE

Symbol	Meaning	Units
B	parameter B, see Eq. (18)	min
C_p	Specific heat of air	kJ/kg K
D	Mass diffusivity	m^2/s
F	Fraction of mist collected at floor	-
k	*Thermal conductivity of air*	*J/ m s K*
L	Latent heat of evaporation of water	kJ/kg
m_d	Droplet mass	kg
m_m	Mass flow rate of mist spray	kg/s
m_{max}	Maximum mist mass flow rate that can evaporate completely	kg/s
q	Rate of heat transfer	W
q_m	Rate of heat transfer with mist	W
r	Droplet radius	m
r_0	Initial droplet radius	m
r_t	Droplet radius at time t	m
t	Time	s
T_∞	Temperature of environment	˚C
t_{ev}	Time to complete droplet evaporation	s
t_s	Mist spraying duration	min
T_s	Temperature of droplet surface	˚C
T_{WB}	Wet bulb temperature	˚C
V_a	Volume flow rate of air	m^3/s
x_o	Absolute humidity of air at initial state	kg/kg'
x_{sat}	Absolute humidity of saturated air for x_0 constant-enthalpy line	kg/kg'
Y	Evaporation fraction of mist spray	-
ΔT_a	Air temperature drop from mist cooling	K
ΔT_{WB}	Wet bulb depression	K
Δx	Change in absolute humidity	kg/kg'
ρ_a	Density of air	kg/m^3
ρ_{da}	Density of dry air	kg/m^3
$\rho_{v,\infty}$	Density of water vapor of environment	kg/m^3
$\rho_{v,s}$	Density of water vapor at droplet surface	kg/m^3
ρ_w	Density of water	kg/m^3

6. ACKNOWLEDGEMENTS

This research was funded by the Osaka City Water Bureau. Nozzles and equipment were provided by Ikeuchi Co., Ltd. The main author is grateful for financial aid from the Japan Student Services Organization during the trial period.

References

(1) Planning Commission for Deployment of Osaka's Waste Incineration Facilities, Osaka-shi gomi shokyakujo seibi – haichi keikaku kentō iinkai hōkokusho (Report of the Planning Commission for Deployment of Osaka City Waste Incineration Facilities.) (2009) [White paper, in Japanese] p.3.
(2) S.Alvarez, E.A.Rodriguez and R.Martin, Direct air cooling from water drop evaporation, Proc. of PLEA'91, Seville, Spain (1991), pp.619-624.
(3) D.Pearlmutter, E.Erell, Y.Etzion, I.A.Meir and H.Di, Refining the use of evaporation in an experimental down-draft cool tower, Energy and Buildings, 23 (1996), pp.191-197.
(4) H.Yamada, G.Yoon, M.Okumiya and H.Okuyama, Study of cooling system with water mist sprayers: Fundamental examination of particle size distribution and cooling effects, Building Simulation, 1(3), (2008), pp.214-222.
(5) S.Uchiyama, K.Suzuki, S.Tsujimoto and H.Koizumi,. Misuto de ekisha no ondo wo sageru kokoromi (An experiment in reducing temperature at a rail platform), Japan Soc. of Plumbing Engineers, 25(2) (2008), pp.8-11.
(6) P.J.O'Rourke, Collective Drop Effects on Vaporizing Liquid Sprays, Ph.D. thesis (1981), Princeton University, United States.
(7) A.Takakura, C.Farnham, K.Masumoto and M.Nakao, Unten deta kara mita ippan haikibutsu shoukyaku setsubi ni okeru hatsuden kouritsu no koujou ni kan suru kentou (Study on increases in power generation efficiency of operation data from a waste-to-energy plant), Proc. 21st Japan Soc. Of Material Cycles and Waste Management Conference (2010), pp. 443-444.
(8) Japan Meteorological Agency. Kako no kishō deta kensaku (Past weather data search), http://www.data.jma.go.jp/obd/stats/etrn/index.php (accessed 2010)
(9) G.vanWylen, R.Sonntag and C.Borgnakke, Fundamentals of Classical Thermodynamics, 4th Ed. New York: John Wiley & Sons, Inc. (1994) p.346.
(10) H.Pruppacher and J.Klett, Microphysics of Clouds and Precipitation, Dordrecht: Kluwer Academic Publishers. (1997), p.490
(11) C.Farnham, M.Nakao, M.Nishioka, M.Nabeshima and T.Mizuno, Misuto no jouhatsu reikyaku tokusei to seigyo houshiki no teian (A Proposal for a Mist Cooling Control and Measurement Methods), Trans. of the JSRAE, 26(1) (2009), pp.105-115.
(12) H.Pruppacher and J.Klett, Ibid. p .397.
(13) A. Lefebvre. Atomization and Sprays. Hemisphere Publishing. (1989), p.311.
(14) D.Lovy *WinDIG* v.2.5. Computer software. (1996) University of Geneva. http://www.unige.ch/sciences/chifi/cpb/ windig.html

(Received Oct. 24, 2012, Accepted Dec. 26, 2012)